Laser-produced rare-earth x-ray spectra*

P. G. Burkhalter, D. J. Nagel, and R. R. Whitlock
Naval Research Laboratory, Washington, D.C. 20375
(Received 29 October 1973)

Laser-produced x-ray spectra of Sm, Gd, and Dy were measured in the energy range 800–2300 eV. Atomic self-consistent-field calculations were used to identify the transitions in ions stripped to the M shell for the Gd spectra. This work extends the Ni I isoelectronic sequence to rare-earth elements.

I. INTRODUCTION

The plasma produced by a high-powered laser contains highly-stripped atoms and is a unique source for atomic spectroscopy. A mode-locked laser with $\sim 10^{10}$ W power generated temperatures in excess of 10^6 °K when focused onto solid targets. Intense radiation from Al, Zn, and Gd ions was found in such plasmas[1] in the 800–3000-eV range. In this work, new M-series x-ray spectra produced by optical-like resonance transitions in highly-ionized rare-earth atoms were identified by use of atomic self-consistent field (SCF) calculations. The most intense rare-earth spectral lines belong to the isoelectronic sequence of Ni I with a ground-state term $3d^{10}\,{}^1S_0$. These spectra are similar to vacuum spark produced uv spectra[2,3] from elements with atomic number about 40 and optical spectra[4–6] from elements with Z about 30.

II. EXPERIMENTAL

The laser system used to produce the plasmas consisted of the mode-locked Nd: YAlG (neodymium: yttrium aluminum garnet) oscillator producing 1.06 μm light, a Pockel's-cell gate which switches out a single pulse with an energy of a few millijoules, two Nd:YAlG preamplifiers, three Nd:glass amplifiers, and a second Pockel's-cell gate used for isolation. The Fabry-Perot etalon in the oscillator cavity yielded pulses of 0.9 nsec. McMahon and Emmett[7] have described the development of this laser system. Pulses from 1 to 20 J of the laser light were focused at nearly normal incidence onto metallic, thick targets by a f-14, 5-cm diameter lens. X-ray calibration lines were obtained from Na, Mg, and Al spectra superimposed on the rare-earth spectra in laser shots with targets coated by thin layers of either Na_2O, MgO, or Al_2O_3 powder. Separate shots were made for each of the three materials overlaying the rare-earth targets. A slitless flat-crystal Bragg spectrograph used a 5-cm long potassium acid phthlate (KAP) diffraction crystal to collect the x-ray spectra. The crystal length in the present experiment cut off the data at about 2300 eV, while the 25 μm Be window used as a light-tight cover over the Kodak No-Screen x-ray film limited measurements to about 800 eV. Each spectrum in this work was obtained with a single laser shot.

III. RESULTS

Laser-produced spectra from Gd were selected for making identifications of ionization states and spectral transitions. Similar x-ray line patterns were found for other laser-produced rare earth spectra for Sm through Yb and also for Ba; however, energy calibrations were made only for Sm, Gd, and Dy. Two different laser-produced spectra for Gd in the 1100–2300 eV energy range are shown in Fig. 1. These spectra are tracings of superimposed, uncorrected densitometer plots. The line energies shown in Fig. 1 for most of the peaks were obtained using a least-square fitting program written for the flat-crystal Bragg spectrograph. The helium- and hydrogen-like resonance lines in the x-ray spectra of Na, Mg, and Al produced by the laser have suitable energies[8] to completely calibrate the spectra for these rare-earth targets. The energies of the calibration lines from the three elements overlapped sufficiently to obtain consistent line energies to an accuracy within ±2 eV over the entire Gd spectrum.

A self-consistent-field (SCF) computer program of Liberman[9] which solves the relativistic Dirac equation by the Hartree-Slater method was used to calculate transition energies for selected electron spin states. In general, SCF calculations yield absolute atomic energies accurate to only 1%–2% (15–30 eV); however, relative energies for different transitions are usually reliable to a few eV and are valuable in identifying x-ray patterns. For instance, relative x-ray line spacings were used to identify spectra emitted by atoms with multiple vacancies produced by high-velocity ions, where computed relative energies

agreed accurately with experimental line spacings.[10] Below the spectra in Fig. 1 are vertical lines corresponding to the calculated transition energies for the two most prominent ionization states; horizontal lines and arrows classify the transitions involved, as will be discussed below. In the spectra for Gd the number of missing electrons ranges from 34 to 38 with the most intense x rays corresponding to ions stripped to the M shell in Gd XXXVII corresponding to the ionization state Gd^{+36}.

Close examination of the spectra in Fig. 1 reveals that higher ionization states are present in the spectrum shown by the solid curve. These spectra were collected with laser energy on target of 1.7 and 4.2 J. A number of Gd shots were made near these power levels. The spectral intensities ranged between those shown but did not correlate with laser power. Plasma temperature and associated ionization states depend on the power density (W/cm^2) on target. The power level was monitored in these experiments but not the focal spot size. Hence we can make no correlation between the spectra (ionization states) and the incident power density at present. In a 20-J shot there was considerable line broadening but no evidence of higher ionization states.

IV. DISCUSSION

The atomic SCF calculations and the intensity differences between spectra produced in different laser shots were used to classify the x-ray lines emanating from highly-stripped rare-earth atoms. In addition, supporting evidence was obtained from extrapolations and other observations of energies of identical transitions in both vacuum spark- and laser-produced uv spectra from lower Z elements.

Prior to the spectral identifications, atomic transition energies were calculated for comparison with known experimental x-ray energies.[11] Adiabatic calculations were performed for normal x-ray lines with single vacancies by taking the difference between total energies computed for initial- and final-state configurations. Calculations were performed for the ordinary L-series x rays of Fe and the M-series x rays of Gd and Au. In addition, calculations for the $2p \rightarrow 3s$ and $2p \rightarrow 3d$ transitions were made and compared to experimental centroids of the multiplet structures in Fe XVIII. The adiabatic calculations were 12–15 eV lower than experimental x-ray line energies for atoms with both single and multiple vacancies. "Sudden-approximation" calculations of transition energies are obtained by taking differences in

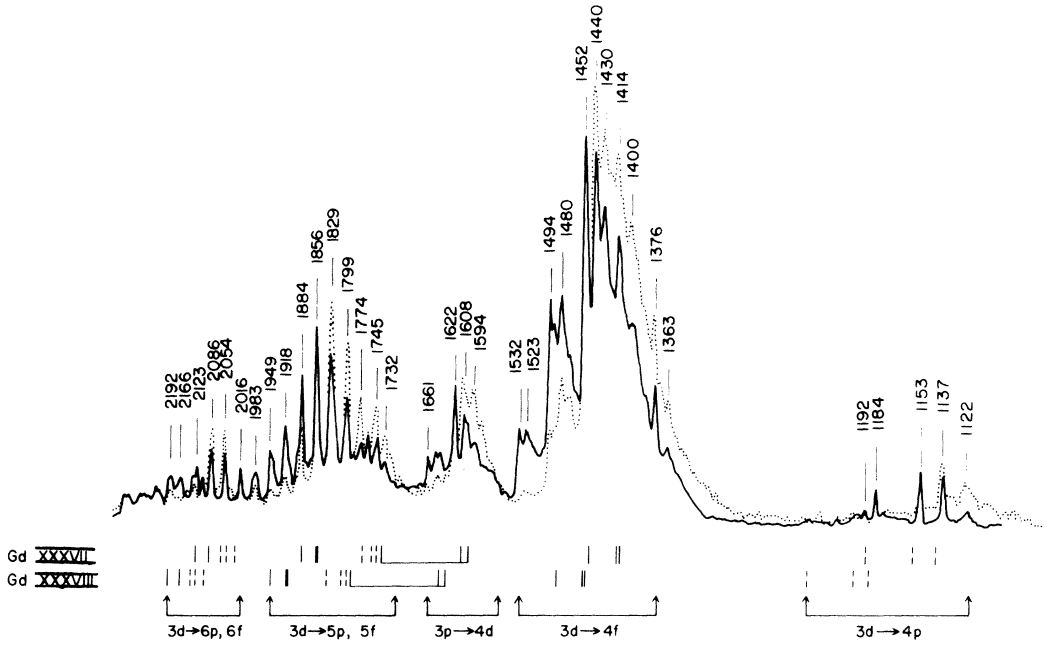

FIG. 1. Laser-produced x-ray spectra for Gd from two different shots. The laser energies were 4.2 and 1.7 J on target for the solid and dotted curves, respectively. The energies in eV of the most prominent peaks in the spectra are given above the x-ray lines. The short vertical marks below the spectra are transition energies calculated by the sudden-approximation method using a SCF program for the two most prominent ionization states. Transitions $3d \rightarrow n_2p$ are indicated by dashed vertical lines, while the other transitions are represented by solid vertical lines. Groups of lines for the same type of transition are indicated in the figure.

binding energies of the initial and final levels. Computer calculations were performed for final-state configurations with full Slater exchange in various Gd ions with between 34 and 42 missing outer electrons. The sudden-approximation method using final configuration computations consistently gave larger values than the adiabatic calculations and these values were in better agreement with the experimental x-ray line energies for the cases tested. Sudden-approximation calculations for stripped Gd gave values 15–19 eV higher than the adiabatic method for transitions between $n_1 = 3$ to $n_2 = 4$ and 13–15 eV higher for $n_1 = 3$ to $n_2 = 5,6$ transitions for both the $3p$ and $3d$ subshells (n_1 and n_2 are the principal quantum numbers of the shells involved in the transition). Therefore the sudden-approximation method provided nearly the correct transition energies. Furthermore, in the sudden-approximation method, calculations for all allowed transitions obeying the selection rules $\Delta L = \pm 1$, $\Delta j = 0, \pm 1$ could be performed with only a few computer runs.

Differences in the intensity for the two spectra in Fig. 1 provided valuable information for interpreting ionization states. Several strong lines were found to have the same intensities in both spectra. Most of the equal intensity lines, e.g., at 1153, 1452, 1622, and 1856 eV, have energies in agreement with calculated energies for Gd^{+36}. In the spectrum from the cooler plasma (dotted line), lower-energy lines and tailing towards lower energies is observed for transitions between the M shell and both the $n_2 = 4, 5$ levels in Gd^{+36}. An energy shift of minus 14 eV from the transition energies for Gd^{+36} was calculated for each $4s$ electron added to Gd ions having a filled M-shell core. Ions with electrons in the numerous subshells outside the $4s$ subshell will have energy shifts of less than the 14-eV shift calculated for ions with $4s$ electrons. Hence the tailing associated with the most intense lines can be ascribed to satellites from lower ionization stages. Low-energy satellites are familiar in K- and L-shell resonance-line spectra. Removal of successive $3d$ electrons corresponding to higher ionization states in $3d^n$ configurations produced energy shifts of about 39 eV towards higher energy. In the $3d - 4f$ transition group, lines which correspond to ionization states Gd^{+37} and Gd^{+38} are found at 1494 and 1532 eV, respectively, in the hotter shot. The SCF calculations of the transition energies by the sudden-approximation method are seen in Fig. 1 to correlate reasonably well the overall observed Gd x-ray spectra from atoms ionized to the M shell.

Let us now look more closely at each transition group identified in Fig. 1.

A. $3d^{10}$-$3d^9 4p$ transitions

In vacuum spark data of lower-Z elements,[2-6] two strong lines and sometimes a weak line at lower energies are found for $3d^{10}$-$3d^9 4p$ transitions in the Ni I isoelectronic sequence. Considering the stronger lines, the $^1S_0$-$^3D_1^0$ transition

TABLE I. Isoelectronic sequence of Ni I.[a]

Element	Transition	Rel. int.[a]	Energy (eV)	Wavelength (Å)
Sm XXXV	$3d^{10}$-$3d^9(^2D_{3/2})4f_{5/2}$		1325 ± 2	9.36 ± 0.02
	-$3d^9(^2D_{5/2})4f_{7/2}$		1289	9.62
	-$3d^9(^2D_{5/2})4f_{5/2}$		1259(?)	9.85
	$3d^{10}$-$3d^9(^2D_{3/2})4p_{3/2}$		1075 ± 2	11.53
	-$3d^9(^2D_{5/2})4p_{3/2}$		1048	11.83
	-$3d^9(^2D_{3/2})4p_{1/2}$		1037	11.95
Gd XXXVII	$3d^{10}$-$3d^9(^2D_{3/2})4f_{5/2}$	100	1452 ± 2	8.54
	-$3d^9(^2D_{5/2})4f_{7/2}$	35	1414	8.77
	-$3d^9(^2D_{5/2})4f_{5/2}$	30	1376(?)	9.01
	$3d^{10}$-$3d^9(^2D_{3/2})4p_{3/2}$	45	1184 ± 2	10.47
	-$3d^9(^2D_{5/2})4p_{3/2}$	60	1153	10.75
	-$3d^9(^2D_{3/2})4p_{1/2}$	40	1137	10.90
Dy XXXIX	$3d^{10}$-$3d^9(^2D_{3/2})4f_{5/2}$		1585 ± 4	7.82
	-$3d^9(^2D_{5/2})4f_{7/2}$		1546	8.02
	-$3d^9(^2D_{5/2})4f_{5/2}$		1497(?)	8.28
	$3d^{10}$-$3d^9(^2D_{3/2})4p_{3/2}$		1300 ± 2	9.54
	-$3d^9(^2D_{5/2})4p_{3/2}$		1264	9.81
	-$3d^9(^2D_{3/2})4p_{1/2}$		1245	9.96

[a] Relative line intensities obtained after correcting crystal efficiency, Be absorption, and film response, but neglecting superposition of intensities from different ionization states for the 1452- and 1137-eV lines in Gd XXXVII.

is about 80% as intense as the $^1S_0$-$^1P_1^0$ transition in Ga IV[5] and in Y XII[3], indicating departure from LS coupling even in the lower-Z members of the isoelectronic series. For Zr XIII[3] the intensity ratio of the two stronger lines is about 3:5, which is the same as observed for the 1153- and 1184-eV lines corresponding to the transitions $3d_{5/2} - 4p_{3/2}$ and $3d_{3/2} - 4p_{3/2}$, respectively, in Gd XXXVII. The notation used for lower-Z work is not carried over into the rare-earth work, but rather the j values for the spin orbitals involved were used because j-j coupling should be prevalent at high atomic numbers. The relative intensity of the weakest line $^1S_0$-$^3P_1^0$ is about 10% of the intensity of the strongest line in this transition group for Ga IV[5] and Y XII[3]. This line in the Gd spectra at 1137 eV agrees with the calculated value for the transition $3d_{3/2} - 4p_{1/2}$ but is too intense to belong solely to Gd XXXVII. Since the intensity of the 1137-eV line is higher in the cooler spectrum and is 16 eV below the 1153-eV line, it is believed to be a satellite line with ionization state Gd^{+35}, while the line at 1122 eV correlates as a $(4s)^2$ satellite line in the ionization state Gd^{+34}. The $3d_{5/2} - 4p_{3/2}$ line for Gd^{+37} is seen at 1192 eV, which agrees with the 39-eV separation for removal of a $3d$ electron. The SCF calculation predicts the relative spacings quite accurately for the $3d - 4p$ transitions. The calculated absolute values in Fig. 1 are about 5 eV too large as expected from a comparison of the adiabatic and nonadiabatic methods with experimental x-ray lines as discussed earlier.

B. $3d^{10}$-$3d^9 4f$ transitions

In the $3d - 4f$ spectral region, Alexander *et al.*[3] report values for two strong lines with the highest energy line being twice the intensity of the other. They also observe a lower-energy weak line in Y XII but not in Zr XIII. Likewise, Edlén[2] observed three lines for $3d^{10}$-$3d^9 4f$ transitions in Rb X but did not report wavelength values. In the Gd spectra strong lines are found at 1452 and 1414 eV, corresponding to the SCF calculations for Gd^{+36}. These have an intensity ratio of about 5:2; however, the 1452-eV line contains intensity from the Gd^{+37} state. The peaks at 1494 and 1532 eV correspond to calculations for ionization states Gd^{+37} and Gd^{+38}, respectively, which are weak in the spectrum for the cooler plasma. At about 14 eV below the energy of these latter two peaks are seen the satellite lines for ions with $4s$ electrons. The strong tailing towards low energy in the $3d - 4f$ region is attributed to superposition of satellite lines for ions containing a few outer subshell electrons in addition to the filled M-shell

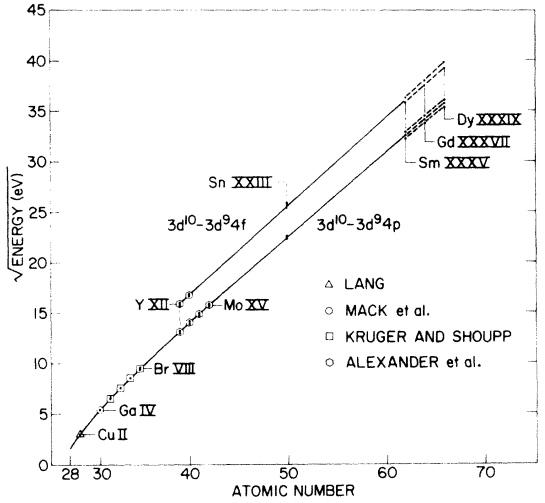

FIG. 2. Moseley plot for Ni I isoelectronic series.

core. The intensity of this satellite structure is greatly enhanced in the spectrum from the cooler plasma. The line at 1376 eV has not been identified by the SCF calculations but has an intensity equal to the 1414-eV line and possibly could be the $3d_{5/2} - 4f_{5/2}$ line that is weak or missing in low-Z spectra. The line at 1376 eV appears to have a satellite line at 1363 eV. In recently acquired laser-produced uv spectra of Sn, there are three distinct lines in the region estimated as $3d^{10}$-$3d^9 4f$ in Sn XXIII. The two lower-energy lines have nearly equal intensity.[12]

The x-ray line energies for the $3d^{10}$-$3d^9 4p$ and $3d^{10}$-$3d^9 4f$ Ni I transitions in Sm, Gd, and Dy are listed in Table I. The square root of the transition energies were plotted as a function of Z in Fig. 2 together with published energies for lower-Z elements and the laser-produced Sn data. Near linearity can be seen in the Moseley plot joining the vacuum spark uv work and the laser-produced Sn and rare-earth spectral data. This supports our identifications that the most intense lines in the rare-earth spectra belong to the Ni I isoelectronic sequence. The degree of linearity for the uv data of Alexander *et al.* and the laser-produced data was investigated. For the most intense line in the $3d^{10}$-$3d^9 4p$ transition a linear least-square fit to the eight data points produced deviations of ± 6 eV for the Sn and rare-earth energies. The deviations for $3d^{10}$-$3d^9(^2D_{5/2})4p_{3/2}$ transition were reduced to ± 2.5 eV with the following quadratic equation:

$$\sqrt{E} = 2.949 + 0.8643\zeta - 0.00071\zeta^2 ,$$

where ζ is the degree of ionization, that is, the ionization state plus one. Likewise the $3d^{10} - 3d^9(^2D_{5/2})4f_{7/2}$ transition energies were fit to

±3.0 eV by the least-squares method, yielding

$$\sqrt{E} = 5.432 + 0.8965\zeta - 0.00073\zeta^2.$$

These equations are nearly linear, in agreement with the Edlén equation (29.1).[2] The coefficient of ζ is about 10% larger than the hydrogenic constant $\sigma^H = 0.8132$ for transitions between $n_1 = 3$ and $n_2 = 4$ levels. These equations can be used as short-range extrapolation formula to calculate transition energies for other rare-earth elements.

C. $3p \rightarrow 4d$ transitions

The next group of lines have been identified as $3p \rightarrow 4d$ transitions because of agreement with SCF calculations. Association of this group of lines with $3d \rightarrow 4f$ transitions in ions with a larger number of $3d$ vacancies than for Gd^{+38} was ruled out because the corresponding $3d \rightarrow 4p$ transitions are missing. Also removal of the more tightly bound $3p$ or $3s$ instead of $3d$ electrons produced calculated shifts in $3d \rightarrow 4f$ transitions of only about 5-eV different from those for $3d$ vacancies. Therefore these lines are not $3d \rightarrow 4f$ transitions in higher ionization states.

The $3p \rightarrow 4d$ transitions have not been identified previously in spark excited uv spectra,[2,3] possibly because of grating restrictions to wavelengths about 45 Å. However, transitions of the type $3p^6 3d^9$-$3p^5 3d^{10}$ are present in the Sn spectrum,[12] confirming ionization of $3p$ electrons. In low-power laser studies of uv spectra from an aluminum plasma, Carillon *et al.*[13,14] have observed transitions involving $2s$ inner-shell vacancies and point out that they are several times more intense than in spark discharges. The high intensity of the $3p \rightarrow 4d$ transitions observed in the Gd spectra and those observed in the Al work indicate that laser plasmas can contain many inner subshell vacancies.

D. $3d \rightarrow n_2 = 5, 6$ transitions

Higher-order levels of Rydberg series lines are common in optical spectra. The group of lines for $n_2 = 5$ transitions have x-ray peaks in correspondence with the SCF calculations, but there is concern about the intensity ratios for the $3d \rightarrow 5f$ to $3d \rightarrow 5p$ transitions. They appear suitable for Gd^{+36} but not for Gd^{+37}. Further experimentation with greater x-ray dispersion in this region should prove interesting. In the group of lines for $n_2 = 6$, the intensity ratio and energy level matching with the SCF calculations is improved if the calculations are shifted such that the first calculated value for Gd^{+36} agrees with the line at 1983 eV. This would yield a pair of lines for $3d \rightarrow 6p$ at 2016 and 1983 eV and a pair of more intense lines for $3d \rightarrow 6f$ at 2086 and 2054 eV.

When configurations contain one or a few electrons with large values of n_2 and l_2 outside almost-closed shells, the atomic levels occur in two groups whose energy separations nearly equal the spin-orbit splitting of the hole in the ion core. The jl(or jK[15]) coupling approximation theoretically predicted exactly the observed levels in the $3d^9 5f$ and $3d^9 5g$ configuration of Cu II.[16] Pairs of lines between 1745 and 2086 eV are observed in the $3d \rightarrow 5p$, $5f$ and $3d \rightarrow 6p$, $6f$ regions in correspondence with the SCF calculations. These have separations of 28–31 eV in the $3d \rightarrow 5p$, $5f$ region, while in the $3d \rightarrow 6p$, $6f$ region line spacings of 32–33 eV are present. A $3d^9 {}^2D_{5/2,3/2}$ spin-orbit splitting of 28.0 eV was calculated by extrapolation of data for $3d^9 4p$ from Alexander *et al.*[3] and a separation of 35.2 eV was calculated in the SCF program for the $3d^9$ core configuration. The separation between absorption edges for atomic Gd is 32.0 eV.[17] The appearance of two line groups for the transitions to outer $n_2 = 5, 6$ levels in the Gd spectra and the separation energies are qualitatively consistent with prior knowledge.

Returning to general considerations applying to all transition groups, we note that various experimental (spectrograph) parameters affect the intensities shown in Fig. 1. These effects include crystal diffraction efficiency, Be window absorption, and film response for various x-ray energies. The largest intensity correction in these Gd spectra is due to the 1-mil Be window absorption. It is about twice as large for the $3d \rightarrow 4p$ transitions as for $3d \rightarrow 4f$ lines. Applying the above intensity correction, the intensity ratio for the 1452–1153-eV ($3d \rightarrow 4f$ to $3d \rightarrow 4p$) lines is reduced to 1.7, in exact agreement with the intensity ratio for the 2086–2016-eV ($3d \rightarrow 6f$ to $3d \rightarrow 6p$) lines for which the intensity correction factors are only about 3%. The intensity agreement for the above line ratios is further support for the identifications that have been made for these lines if the relative excitation probabilities to empty p-like and f-like orbitals are independent of principal quantum numbers.

The highest x-ray energies observed thus far at NRL with single-pulse laser shots have been about 3 keV. Using the Moseley diagram for extrapolation of x-ray energies, one can estimate how high in atomic number laser-produced M spectra might be expected. The Z range for x-ray spectra from the $n_2 = 4$ levels with single-laser pulses in the range 1–20 J on target would extend to about $Z = 85$. Higher laser powers and the use of prepulses should permit extension of the Ni I se-

quence through uranium.

The present work forms the basis for use of x-ray spectra from high-Z atoms as a diagnostic tool in high-temperature plasmas. Estimates of electron temperatures in plasmas have been made from the ratio of He-like to H-like line intensities in lower-Z elements like Al.[18] Since a larger number of ionization states have been identified in the Gd spectra compared to low-atomic-number elements, refinements in temperature determinations are potentially possible but must await calculations of excitation probabilities for high-Z elements. However, some plasma-diagnostics experiments, including correlation of ionization states in high-Z elements with laser-power density can be made now.

In conclusion, the over-all pattern of x-ray lines found in rare-earth spectra produced by a high-power laser involve (i) resonance transitions from the $n_2 = 4, 5, 6$ levels to the M-shell in highly stripped atoms, (ii) strong satellite lines for atoms not completely stripped to the M-shell, and (iii) transitions to $3p$ inner subshell vacancies. The most distinct ionization state is isoelectronic with Ni I. The entire Ni I series can probably be completed with laser-produced spectra.

ACKNOWLEDGMENTS

The authors are grateful to U. Feldman for calibration of the Sn spectrogram and J. W. Criss for computer assistance in the x-ray film calibrations.

---

*Work done under the auspices of the Defense Nuclear Agency.

[1]D. J. Nagel *et al.* (unpublished).

[2]B. Edlén, *Handbuch der Physik*, edited by S. Flügge (Springer, Berlin, 1964), Vol. XXVII, pp. 80–220.

[3]E. Alexander, M. Even-Zohar, B. S. Fraenkel, and S. Goldsmith, J. Opt. Soc. Am. 61, 508 (1971).

[4]R. J. Lang, Phys. Rev. 31, 773 (1928).

[5]J. E. Mack, O. Laporte, and R. J. Lang, Phys. Rev. 31, 748 (1928).

[6]P. G. Kruger and W. E. Shoupp, Phys. Rev. 46, 124 (1934).

[7]J. M. McMahon and J. L. Emmett, in *Record of Eleventh Symposium on Electron, Ion, and Laser Beam Technology*, edited by R. F. M. Thornley (San Francisco Press, San Francisco, 1971).

[8]R. L. Kelly, in *Atomic Emission Lines Below 2000 Å Hydrogen through Argon*, NRL Report 6648 (U.S. GPO, Washington, D.C., 1968).

[9]D. Liberman, J. T. Waber, and D. T. Cromer, Phys. Rev. 137, A27 (1965).

[10]A. R. Knudson, D. J. Nagel, P. G. Burkhalter, and K. L. Dunning, Phys. Rev. Lett. 26, 1149 (1971).

[11]J. A. Bearden *et al.*, U.S. AEC Report No. NYO-10586, pp. 533 (1964).

[12]P. G. Burkhalter *et al.* (unpublished).

[13]A. Carillon, G. Jamelot, A. Sureau, and P. Jaegle, Phys. Lett. A 38, 91 (1972).

[14]A. Carillon, P. Jaegle, G. Jamelot, and A. Sureau, in *Proceedings of the International Conference on Inner-Shell Ionization Phenomena* (U.S. AEC, Atlanta, Ga. 1973), Vol. 4, p. 2373.

[15]R. D. Cowan and K. L. Andrew, J. Opt. Soc. Am. 55, 502 (1965).

[16]G. H. Shortley and B. Fried, Phys. Rev. 54, 749 (1938).

[17]J. A. Bearden and A. F. Burr, Rev. Mod. Phys. 39, 125 (1967).

[18]B. M. Klein, C. M. Dozier, D. J. Nagel, and R. R. Whitlock, Variation of the Temperature of Laser-Produced Plasma with Laser Pulse and Target Parameters, presented at European Conference on Controlled Fusion and Plasma Physics, Moscow, 1973 (unpublished).